Dyes and Pigments 105 (2014) 1–6

Contents lists available at ScienceDirect

Dyes and Pigments

journal homepage: www.elsevier.com/locate/dyepig

Effect of different acceptors in di-anchoring triphenylamine dyes on the performance of dye-sensitized solar cells

Guohua Wu [a], Fantai Kong [a,*], Yaohong Zhang [b], Xianxi Zhang [c], Jingzhe Li [a], Wangchao Chen [a], Changneng Zhang [a], Songyuan Dai [d,a,*]

[a] Key Laboratory of Novel Thin Film Solar Cells, Institute of Plasma Physics, Chinese Academy of Sciences, Hefei 230031, PR China
[b] Key Laboratory of Optoelectronic Materials Chemistry and Physics, Fujian Institute of Research on the Structure of Matter, Chinese Academy of Sciences, Fuzhou 350002, PR China
[c] Shandong Provincial Key Laboratory of Chemical Energy Storage and Novel Cell Technology, School of Chemistry and Chemical Engineering, Liaocheng University, Liaocheng 252059, PR China
[d] School of Renewable Energy, North China Electric Power University, Beijing 102206, PR China

A R T I C L E I N F O

Article history:
Received 6 December 2013
Received in revised form
6 January 2014
Accepted 10 January 2014
Available online 22 January 2014

Keywords:
Di-anchoring triphenylamine dye
Dye-sensitized solar cells
Organic sensitizer
Photovoltaic performance
Electrochemical impedance spectroscopy
Electron acceptor

A B S T R A C T

Three di-anchoring triphenylamine dyes, which were coded as **TPAC1**, **TPAR2** and **TPACR2**, were designed and synthesized for dye-sensitized solar cell application. The structural modification effect of different anchoring groups on photophysical, electrochemical and photovoltaic properties of the related DSSCs was extensively investigated. With the variation from cyanoacetic acid via rhodanine-3-acetic acid to co-rhodanine units, the molar extinction coefficients of the maximum absorption wavelength for the three dyes gradually increase due to the extension of π system. In comparison with that for **TPAC1** and **TPAR2**, DSSC based on dye **TPACR2** with double co-rhodanine groups shows the best overall conversion efficiency of 4.64% with simultaneous enhancement of photocurrent and photovoltage, which is attributed to the higher molar extinction coefficient (6.5×10^4 M^{-1} cm^{-1}), broader absorption spectra, broader IPCE spectra and longer electron lifetime.

1. Introduction

As a crucial component in dye-sensitized solar cells (DSSCs), the metal-free organic dyes have always attracted increased attention in the past decades by virtue of their ease of inexpensive synthesis, generally high molar extinction coefficients and tunable absorption spectral response. In the last decade, numerous investigations organic dyes, such as indoline [1–3], coumarin [4,5], cyanine [6–8], perylene [9,10], triphenylamine [11–14], carbazole [15–17], tetrahydroquinoline [18,19], phenothiazine [20–23], phenoxazine [24,25] and fluorene dyes [26,27], have been investigated. So far, organic sensitizers have gained promising overall conversion efficiencies [1,11] (η), which is comparable to ruthenium-based complexes.

By far, most typical metal-free organic dye sensitizers contain a structure of "Donor (D)–conjugated bridge (π)–Acceptor (A)". In order to utilize the sun light as much as possible, two common structural strategies, incorporating more donor segments or enlarging π-conjugated linker into the D–π–A configuration to form the D–D–π–A or D–π–π–A structure, have been considered [28–32]. However, the complexity in the process of synthesis is the major problem. Different from donor and conjugated bridge segments, the electron acceptor (A) carries a polar carboxylic acid as anchoring group to TiO_2 surface. Varying the numbers of anchor groups via protonation state to tune the interfacial electron transfer or photovoltaic properties is very important for Ru-sensitizers. Especially, di-anchoring N719 dye gives higher cell efficiency than the protonated N3 dye with quadri-anchoring groups, which is attributed to the effect of the bound dye on the energy of the TiO_2 conducting band [33]. Similar to Ru-sensitizers, the notion of incorporating double electron acceptor units into the organic donor framework to form di-anchoring dye has been proposed to further enhance the binding strength of dyes on the TiO_2. Several di-anchoring organic dyes, which have been

* Corresponding authors. Key Laboratory of Novel Thin Film Solar Cells, Institute of Plasma Physics, Chinese Academy of Sciences, 350 Shushanhu Road, P.O. Box: 1126, Hefei 230031, Anhui, PR China. Tel.: +86 551 65593222.
E-mail addresses: kongfantai@163.com (F. Kong), sydai@ipp.ac.cn (S. Dai).

0143-7208/$ – see front matter © 2014 Elsevier Ltd. All rights reserved.
http://dx.doi.org/10.1016/j.dyepig.2014.01.012

designed and synthesized for use in DSSCs, have demonstrated better cell performance than mono-anchoring D–π–A sensitizers with an improved photocurrent due to the extension of the π-conjugated system and the enhanced molar extinction coefficient [34–40]. Because the electrons from the photoexcitation of the dye molecules are injected to conduction band of the semi-conductor through the electron acceptor parts, changes in the electron acceptor of the dye sensitizers can result in a significant variation of electronic and photovoltaic properties. As regards acceptor parts, cyanoacetic acid and rhodanine-3-acetic acid generally carried anchoring group to TiO_2 surface in the single D–π–A sensitizers which were discussed in previous work [41–43]. In addition, due to the strong electron withdrawing ability and the extension of the π-conjugation framework, co-rhodanine unit have also been successfully utilized for the application of DSSCs [1,3]. However, the contributions of different electron acceptors in di-anchoring dyes on the electronic and photovoltaic properties have not been well explored. Recently, we present three di-anchoring dyes comprised a triphenylamine group as an electron donor, which are coded as **TPAC1**, **TPAR2** and **TPACR2**. The three di-anchoring dyes were designed to have double electron acceptors (cyanoacetic acid, rhodanine-3-acetic acid, co-rhodanine unit), which are shown in Fig. 1. With the variation from cyanoacetic acid via rhodanine-3-acetic acid to co-rhodanine units, a π-conjugated extension of electron acceptor in di-anchoring organic sensitizers was observed for expanding the possibility of enhancing the optical and photovoltaic properties of the sensitizers. In our study, in comparison with cyanoacetic acid or rhodanine-3-acetic acid, the sensitizer with double co-rhodanine units as the anchor group exhibited the best overall conversion efficiency with simultaneous enhancement of photocurrent and photovoltage.

2. Experimental section

2.1. Materials

Tetrabutylammonium perchlorate (TBAP), 4-tert-butylpyridine (TBP), lithium iodide (LiI) and iodine (I_2) were purchased from Aldrich and used as received. The starting materials triphenylamine and (Z)-2-(2-(3-octyl-4-oxo-2-thioxothiazolidin-5-ylidene)-4-oxothiazolidin-3-yl) acetic acid was purchased from chemsolarism company. All the other solvents and the chemicals are puriss grade and used without further purification.

2.2. Synthesis

In order to investigate the structural modification of different electron acceptor groups upon the photophysical, electrochemical and photocurrent density–voltage characteristics of the DSSCs, double electron acceptor groups were applied into the three dyes with triphenylamine electron donor. The synthetic route of **TPAC1**, **TPAR2** and **TPACR2** dyes is shown in Fig. 1. **DFTPA** and **TPAR2** were synthesized according to the corresponding literature methods [44]. The final step was a Knoevenagel reaction between the carbaldehyde and two equivalent of different electron acceptors (cyanoacetic acid, rhodanine-3-acetic acid or (Z)-2-(2-(3-octyl-4-oxo-2-thioxothiazolidin-5-ylidene)-4-oxothiazolidin-3-yl) acetic acid) in the presence of ammonium acetate in acetic acid.

2.2.1. Synthesis of *TPAC1*

A 25 mL acetic acid solution of **DFTPA** (151 mg, 0.5 mmol), cyanoacetic acid (85 mg, 1.0 mmol) and ammonium acetate (20 mg, 0.26 mmol) was refluxed for 6 h under argon atmosphere. After cooling to room temperature, the precipitate was filtered and washed by distilled water. The crude product was purified by column chromatography (methylene chloride/methanol = 10/1) to obtain **TPAC1** (200 mg, 92%) as a red solid. ^{1}H NMR (500 MHz, $CDCl_3$): δ/ppm: 7.86 (s, 1H, CH), 7.84 (s, 1H, CH), 7.36 (t, 2H, J = 7.5 Hz, ArH), 7.23 (t, 1H, J = 8.5 Hz, ArH), 7.28 (d, 2H, J = 8.5 Hz, ArH), 7.15 (d, 4H, J = 8.0 Hz, ArH), 7.00 (d, 2H, J = 8.0 Hz, ArH). ^{13}C NMR (125 MHz, $CDCl_3$): δ/ppm: 151.5, 145.7, 144.9, 133.8, 132.7, 129.5, 127.7, 126.2, 125.8, 125.4, 119.4, 116.5. MALDI-TOF-MS (m/z): calcd for $(M-2H)^-$ $C_{26}H_{15}O_4N_3$: 433.1063, found: 433.1093.

2.2.2. Synthesis of *TPACR2*

The same procedure as for **TPAC1** but with (Z)-2-(2-(3-octyl-4-oxo-2-thioxothiazolidin-5-ylidene)-4-oxothiazolidin-3-yl) acetic acid (160 mg, 0.4 mmol) were used. The crude product was purified by column chromatography (methylene chloride/methanol = 10/1) to obtain **TPACR2** (150 mg, 70%) as a red solid. ^{1}H NMR (500 MHz, $CDCl_3$): δ/ppm: 7.78 (s, 1H, CH), 7.76 (s, 1H, CH), 7.54 (d, 2H, J = 8.5 Hz, ArH), 7.40 (t, 2H, J = 7.7 Hz, ArH), 7.26 (t, 1H, J = 7.5 Hz, ArH), 7.18 (d, 8H, J = 8.0 Hz, ArH), 4.76 (s, 4H, CH_2), 4.06 (t, 4H,

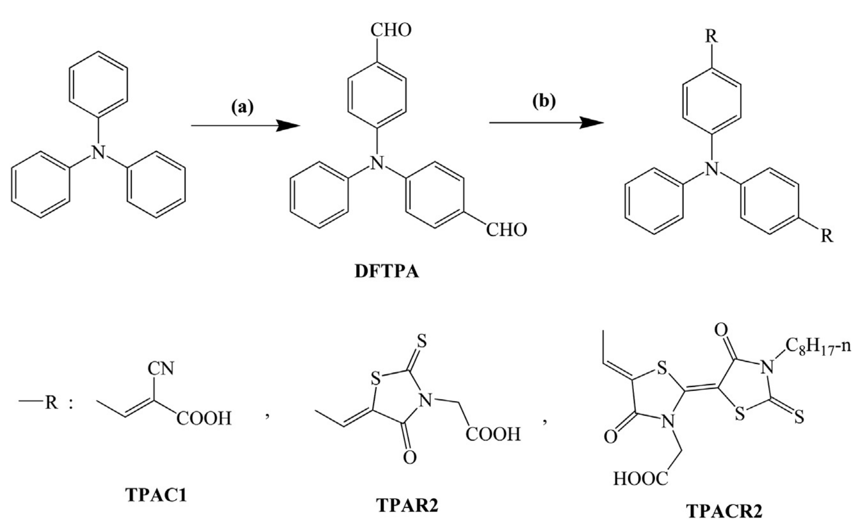

Fig. 1. The synthetic route of the three dyes (**TPAC1**, **TPAR2** and **TPACR2**). (a) $POCl_3$, DMF, reflux, 5 h; (b) cyanoacetic acid, rhodanine-3-acetic acid or (Z)-2-(2-(3-octyl-4-oxo-2-thioxothiazolidin-5-ylidene)-4-oxothiazolidin-3-yl) acetic acid, ammonium acetate, acetic acid, reflux, 6 h.

$J = 8.0$ Hz, CH_2), 1.67 (m, 4H, CH_2), 1.36–1.24 (m, 20H, CH_2), 0.87(t, 6H, $J = 2.5$ Hz, CH_3). ^{13}C NMR (125 MHz, $CDCl_3$): δ/ppm: 190.5, 172.2, 169.0, 166.8, 149.2, 148.0, 144.9, 143.7, 133.8, 132.0, 131.0, 129.7, 126.5, 123.3, 121.6, 117.1, 94.6, 44.7, 44.4, 31.3, 29.2, 28.7, 26.4, 22.2, 13.6. MALDI-TOF-MS (m/z): calcd for $(M)^-$ $C_{52}H_{55}O_8N_5S_6$: 1069.2375, found: 1069.1925.

2.3. Fabrication and characterization of DSSCs

The dye-sensitized TiO_2 electrodes were prepared by following the procedure reported in the literature [45]. Briefly, a double layer of TiO_2 particles ($\sim$10 μm) was screen-printed on the fluorine tin oxide (FTO) coated glass (12–14 Ω per square, TEC 15, USA). After that, the TiO_2 thin-film electrodes were sintered at 450 °C for 30 min and used as the photoelectrode. After cooling to room temperature, the TiO_2 thin-film electrodes were immersed in a $CHCl_3$ solvent containing 3×10^{-4} mol L^{-1} dye sensitizers for at least 15 h, then rinsed with anhydrous $CHCl_3$ and dried. To prepare the counter electrode, Pt catalyst was deposited on FTO glass by spraying H_2PtCl_6 solution and pyrolysis at 410 °C for 20 min. The DSSCs used for photovoltaic measurements consist of a dye-adsorbed TiO_2 working electrode, a 45 μm thermal adhesive film (Surlyn®, USA), an organic electrolyte and a counter electrode. The organic electrolyte solution was a mixture of 0.6 M 1, 2-Dimethyl-3-propylimidazolium iodide (DMPII), 0.1 M LiI and 0.1 M I_2 in acetonitrile or 0.6 M DMPII, 0.1 M LiI, 0.1 M I_2 and 0.5 M TBP in acetonitrile. The area of the TiO_2 film electrodes was 0.25 cm^2.

2.4. Equipments

Absorption spectra were performed on a U-3900H UV–Vis spectrophotometer (Hitachi, Japan). Emission spectra were obtained from the F-7000 spectrofluorimeter (Hitachi, Japan). The oxidation potentials of the three dyes adsorbed on TiO_2 films were measured in a three-electrode electrochemical cell with a CHI-660d electrochemical analyzer (CH Instruments, Inc., China). TiO_2 films stained with the sensitizers were used as working electrodes. Pt wire was used as the auxiliary electrode and Saturated Calomel Electrode (SCE) was used as reference electrode. The supporting electrolyte was 0.1 M tetrabutylammonium perchlorate (TBAP) with dimethylformamide (DMF) as the solvent. The scan rate was 100 mV s^{-1}. Electrochemical impedance spectroscopy (EIS) measurements of the DSSCs were performed using an AUTOLAB PGSTAT 302N analyzer (Metrohm, Switzerland) in the frequency region from 50 mHz to 1000 kHz. The applied voltage bias is −0.55 V. The photocurrent density–photovoltage (J–V) curves of the DSSCs were obtained using a 3A grade solar simulator (Newport, USA, 94043A) under AM 1.5 (100 mW cm^{-2}) illumination. The incident monochromatic photon-to-current conversion efficiency (IPCE) spectra were measured as a function of wavelength from 300 to 900 nm, which was recorded on QE/IPCE measurement kit (Newport, USA).

3. Results and discussion

3.1. Absorption spectra

The absorption spectra of the three dyes **TPAC1**, **TPAR2** and **TPACR2** in diluted solution of $CHCl_3$ (3×10^{-5} M) are shown in Fig. 2. The data are listed in Table 1. The absorption spectra of the three dyes **TPAC1**, **TPAR2** and **TPACR2** in $CHCl_3$ display two distinct absorption bands at around 300–395 nm and 400–600 nm, respectively. The weak absorption peaks in the UV band correspond to the π–π^* electron transition and the strong absorption peaks in the visible band can be assigned to an intramolecular charge transfer (ICT) between the triphenylamine donor and the electron acceptor. The absorption peak values are in the order of **TPACR2** (535 nm) > **TPAR2** (497 nm) > **TPAC1** (426 nm). Note that the above two absorption bands are also red-shifted with the variation from cyanoacetic acid via rhodanine-3-acetic acid to co-rhodanine units. The bathochromic shift which is desirable for harvesting light from the solar spectrum should be assigned to the extension of π system. All the molar extinction coefficients of the maximum absorption wavelength for the three dyes obviously increase with the variation from cyanoacetic acid via rhodanine-3-acetic acid to co-rhodanine units. The higher molar extinction coefficient for **TPACR2** (6.5×10^4 M^{-1} cm^{-1}) compared with that for **TPAC1** and **TPAR2** indicates a good ability for light harvesting.

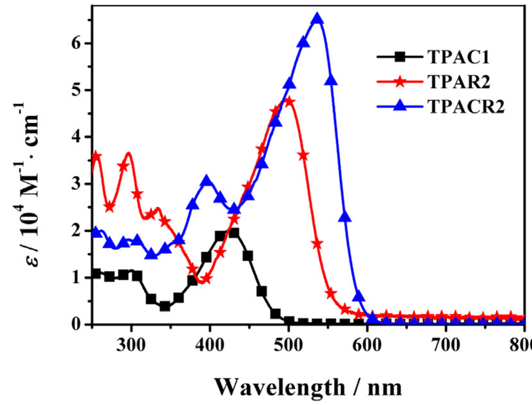

Fig. 2. The absorption spectra of dyes **TPAC1**, **TPAR2** and **TPACR2** in $CHCl_3$ solutions (3×10^{-5} M).

Fig. 3 shows the normalized absorption spectra of the three dyes on 2.5 μm thick TiO_2 films after 12 h adsorption. Compared with the spectra in $CHCl_3$ solution, a blue-shift of the absorption spectra was observed in the two dyes **TPAC1** (20 nm) and **TPAR2** (6 nm) on TiO_2 surface, which can be attributed to the strong interactions between the two dyes and the semiconductor surface especially the formation of H-type aggregation. Furthermore, **TPAC1** dye has larger blue-shifted value as compared to **TPAR2** dye, indicating that **TPAC1** dye has a more tendency to aggregate on TiO_2. However, the absorption spectrum of **TPACR2** on TiO_2 film shows no difference in comparison with that in solution indicating the dye has no tendency to aggregate, which is attributed to the presence of the octyl substituted rhodanine ring.

Table 1
UV–Vis, emission and electrochemical data.

Dye	Abs λ^{a}_{max}/nm (ε^{b}/M^{-1} cm^{-1})	Em λ^{a}_{ex}/ nm	λ^{c}_{max}/ nm on TiO_2	$E^0_{(S+/S)}$[d]/ V (vs NHE)	E_{0-0}[e]/ V (Abs/ Em)	$E^0_{(S+/S^*)}$[f]/ V (vs NHE)
TPAC1	426 (2.0×10^4)	568	406	1.34	2.58	−1.24
TPAR2	497 (4.8×10^4)	577	491	1.25	2.17	−0.92
TPACR2	535 (6.5×10^4)	612	535	1.37	2.14	−0.77

[a] Absorption and emission peaks were measured in $CHCl_3$ solution (3.0×10^{-5} mol L^{-1}) at room temperature.
[b] The molar extinction coefficient at corresponding wavelength of the absorption spectra.
[c] Absorption maximum on TiO_2.
[d] Oxidation potentials of the three dyes adsorbed on TiO_2 films were measured in DMF containing 0.1 mol L^{-1} TBAP with a scan rate of 100 mV s^{-1}, NHE: standard hydrogen electrode.
[e] E_{0-0} transition energy, estimated from the intersection between the absorption and emission spectra in $CHCl_3$ solution.
[f] The $E^0_{(S+/S^*)}$ of the three dyes were calculated from $E^0_{(S+/S)} - E_{0-0}$.

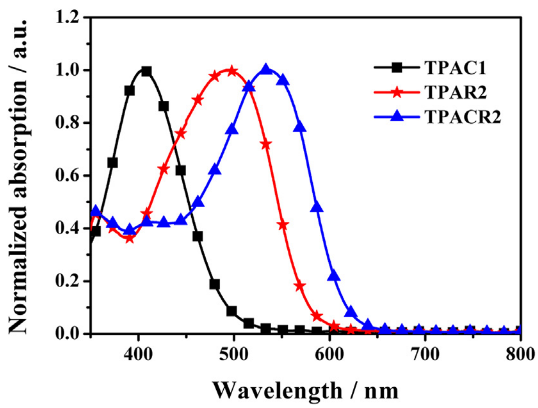

Fig. 3. The normalized absorption spectra of these dyes on the TiO_2 films.

3.2. Electrochemical properties

Electrochemical properties of **TPAC1**, **TPAR2** and **TPACR2** were investigated by cyclic voltammetry in dimethylformamide (DMF) solution containing 0.1 M tetrabutylammonium perchlorate (TBAP) as supporting electrolyte. Fig. 4 shows the cyclic voltammetry curves of **TPAC1**, **TPAR2** and **TPACR2** adsorbed on TiO_2 films and the results were summarized in Table 1. It is shown that the HOMO ($E^0_{(S+/S)}$) levels of **TPAC1**, **TPAR2** and **TPACR2** were sufficiently more positive than the iodine/triiodide redox potential value (0.4 V vs. NHE), ensuring that there is enough driving force for the dye regeneration reaction. On the other hand, the estimated excited state potential ($E^0_{(S+/S^*)}$) corresponding to the LUMO levels of **TPAC1**, **TPAR2** and **TPACR2**, calculated from $E^0_{(S+/S)} - E_{0-0}$, are −1.24 V, −0.92 V and −0.77 V, respectively. It is obvious that the LUMO level of the dye is increased with the increase of the unit of rhodanine ring leading to the smaller driving force. More importantly, the LUMO levels of the three dyes are more negative than the conduction band of TiO_2 (−0.5 V), indicating that the electron injection process from the excited dye molecule to the conduction band of TiO_2 is energetically permitted. From these values, we can clearly conclude that these organic dyes could be used as sensitizers in DSSCs.

3.3. Theoretical calculations

To investigate the molecular structure and electron distribution of the three organic dyes, the three dyes have been optimized using DFT calculations with Gaussian 09 program [46]. The calculations

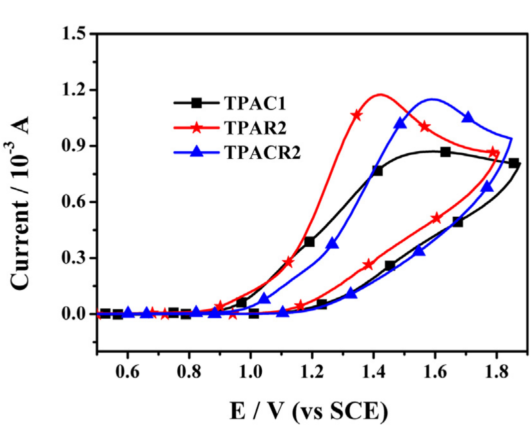

Fig. 4. The cyclic voltammetry plots of **TPAC1**, **TPAR2** and **TPACR2** attached to nanocrystalline TiO_2 films deposited on conducting FTO glass.

were performed with the B3LYP exchange correlation functional under 6-31G (d) basis set. Fig. 5 shows the frontier molecular orbitals of the three dyes. It can be seen that for **TPAC1**, **TPAR2** and **TPACR2**, the HOMO electron density geometry distributions are all over the whole molecular structures especially in the conjugated systems. Neglecting the unsubstituted benzene ring, the LUMO electron density geometry distributions for the three dyes are also all over the whole molecular structures. Furthermore, the LUMO electron density geometry distribution of **TPAR2** and **TPACR2** is mainly concentrated on the rhodanine framework, especially on the carbonyl and thiocarbonyl. In spite of this, the electrons which are generated upon photoexcitation in the three organic dyes anchored onto the TiO_2 film surface, can be successively transferred from triphenylamine to electron acceptor group (cyanoacetic acid group, rhodanine-3-acetic acid group or co-rhodanine group) and finally into the conduction band of TiO_2.

3.4. Photovoltaic performances of DSSCs

The incident photon-to-current conversion efficiency (IPCE) spectra of the cells based on the three dyes and N719 are shown in Fig. 6. The solar cell based on **TPACR2** shows high IPCE above 60% in the range of 390–630 nm and with the highest value of 74% at 570 nm. For the other two dyes sensitized solar cells, the IPCE reaches maxima of 69% at 570 nm for **TPAR2** and 77% at 450 nm for **TPAC1**, respectively. On the other hand, the onset of IPCE for **TPACR2** and **TPAR2** is extended to 690 nm and 640 nm, which corresponds to red shifts of 100 nm and 50 nm respectively in comparison with **TPAC1**. Consistent with their absorption spectra in $CHCl_3$ solvent and on the transparent TiO_2 films, the broader IPCE values for the **TPACR2**-based DSSC may be attributed to its broader absorption, which leads to a higher short circuit photocurrent density compared with that of **TPAC1** and **TPAR2**. Furthermore, the onsets of IPCE spectra for the three dyes are significantly broadened compared to their absorption spectra in solution, which is observed

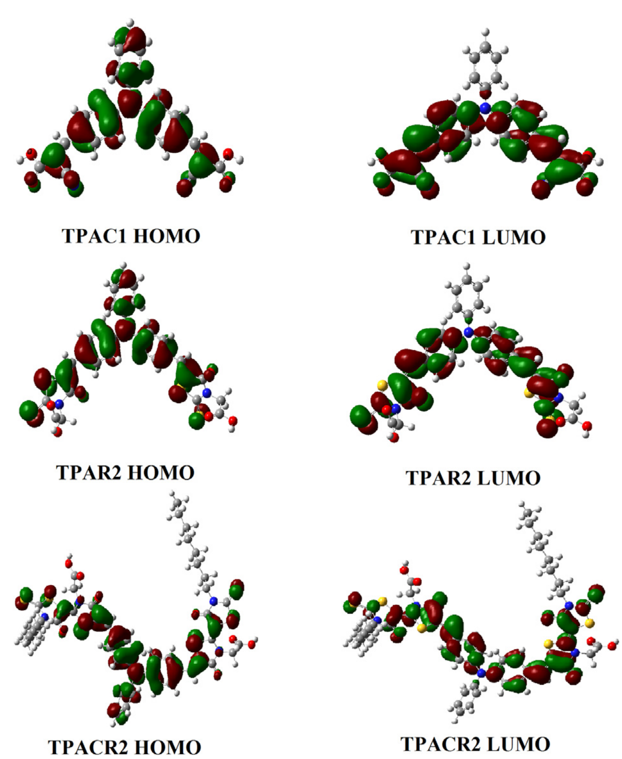

Fig. 5. Molecular orbital distributions of **TPAC1**, **TPAR2** and **TPACR2**.

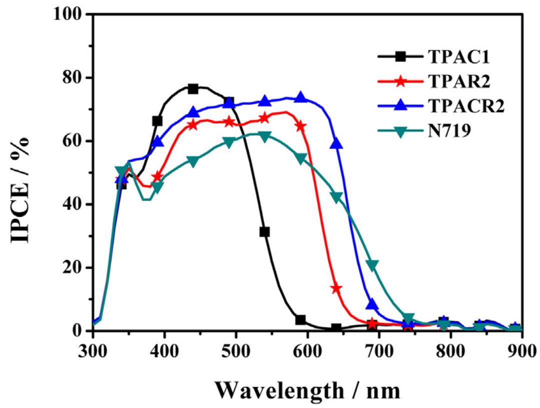

Fig. 6. The IPCE spectra of the DSSCs sensitized with **TPAC1**, **TPAR2** and **TPACR2** dyes.

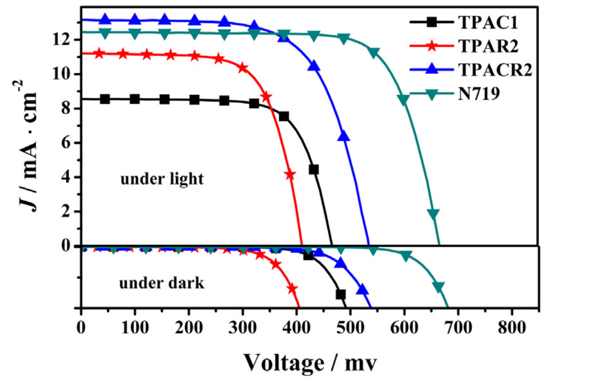

Fig. 7. Current density–voltage curves of the DSSCs sensitized with **TPAC1**, **TPAR2** and **TPACR2** under light (100 mW cm^{-2}, AM 1.5 irradiation) and dark conditions.

for other dyes [5,21,22,26,41]. The exact reason still needs further studies. Here, red shift of the onsets in IPCE spectra for the DSSC based on the three dyes may be attributed to the interaction of Li^+ ions adsorbing on the TiO_2 film from electrolyte solution with the carbonyl group in the dye [5].

Photovoltaic performances of the **TPAC1**, **TPAR2** and **TPACR2** sensitized TiO_2 film electrodes with a liquid electrolyte are listed in Table 2 under AM 1.5 solar simulator illumination (100 mW cm^{-2}), and the corresponding photocurrent density (J)–voltage (V) curves for the DSSCs based on the three dyes are shown in Fig. 7. The **TPACR2** sensitized cell gave an overall conversion efficiency (η) of 4.64% with a short circuit photocurrent density (J_{sc}) of 13.16 mA cm^{-2}, an open circuit voltage (V_{oc}) of 534 mV and a fill factor (FF) of 0.66. Under the same conditions, the **TPAC1** and **TPAR2** sensitized cells gave J_{sc} values of 8.56 and 11.21 mA cm^{-2}, V_{oc} of 467 and 411 mV and FF of 0.71 and 0.68, corresponding to η values of 2.86% and 3.15%, respectively. Evidently, **TPACR2** shows better solar cell performance than **TPAC1** and **TPAR2**, especially in J_{sc} and V_{oc}. Consistent with the trend of the photocurrent integrated from the IPCE spectra, the remarkably enhanced J_{sc} value of the **TPACR2**-based DSSC may be attributed to its higher and broader absorption in comparison with **TPAC1**- and **TPAR2**-based DSSCs. The lower V_{oc} of the DSSCs observed with the three new dyes may be attributed to a faster recombination rate between the injected electrons and I_3^- in electrolytes in comparison to that for N719 dye, which can be seen clearly from the dark currents in J–V test. This result strongly suggests that co-rhodanine unit can be an excellent electron acceptor system for organic dyes to improve the photovoltaic performance.

3.5. EIS analysis

Electrochemical impedance spectroscopy (EIS) measurements were performed to characterize the charge transfer resistances of the cells. Fig. 8 showed the electrochemical impedance spectra for the DSSCs based on the three sensitizers (**TPAC1**, **TPAR2** and **TPACR2**) under a forward bias of −0.55 V in the dark. Three semicircles located in the high-, middle- and low-frequency regions were observed in the Nyquist plots, which are attributed to the charge transfer at the Pt/electrolyte interface, the electron transport at the TiO_2/dye/electrolyte interface and Warburg diffusion process of I^-/I_3^- in the electrolyte, respectively. It is obvious that the radius of the middle semicircle (R_{ct}) is decreased in the order of **TPACR2** (40 Ω) > **TPAC1** (17 Ω) > **TPAR2** (6 Ω) implying the acceleration of the charge recombination between injected electrons and I_3^- in the electrolyte (**TPACR2** < **TPAC1** < **TPAR2**), with a consequent increase of the dark currents for the three dyes observed in J–V test. The electron lifetimes of **TPAC1**, **TPAR2** and **TPACR2** are obtained with 8 ms, 4 ms and 31 ms, respectively. Therefore, the larger charge recombination resistance and enhanced electron lifetime may be the intrinsic reason for the higher V_{oc} value of the DSSC based on **TPACR2** compared to that for the **TPAC1** and **TPAR2**.

Table 2
Photovoltaic performance of DSSCs with the three dyes.[a]

Dye	J_{sc}/mA cm^{-2}	V_{oc}/mV	FF	η/%
TPAC1[b]	8.56	467	0.71	2.86
TPAR2[b]	11.21	411	0.68	3.15
TPACR2[b]	13.16	534	0.66	4.64
N719[c]	12.47	667	0.74	6.17

[a] Irradiating light: simulated AM 1.5 irradiation (100 mW cm^{-2}); working area: 0.25 cm^2.
[b] The electrolyte was a solution of 0.6 M DMPII, 0.1 M LiI and 0.1 M I_2 in acetonitrile.
[c] The electrolyte solution was a mixture of 0.6 M DMPII, 0.1 M LiI, 0.1 M I_2 and 0.5 M TBP in acetonitrile.

4. Conclusions

In summary, three di-anchoring dyes **TPAC1**, **TPAR2** and **TPACR2**, comprised the same donor unit and double different electron acceptors, were synthesized for dye-sensitized solar cells. The absorption spectra are red-shifted with the variation from cyanoacetic acid via rhodanine-3-acetic acid to co-rhodanine units. Among the three dyes, photovoltaic performance of the device with **TPACR2** dye showed a higher overall conversion efficiency of 4.64%

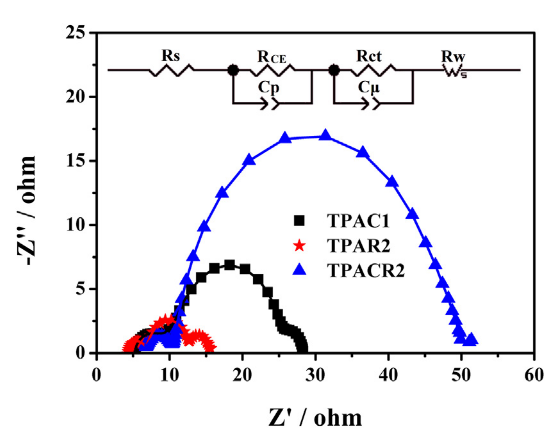

Fig. 8. EIS Nyquist plots for DSSCs based on **TPAC1**, **TPAR2** and **TPACR2** under dark. The inset shows the equivalent circuit.

under simulated AM 1.5 solar irradiation (100 mW cm^{-2}), which were attributed to the higher molar extinction coefficient, broader absorption spectra, broader IPCE spectra and longer electron lifetime. The result strongly suggests that co-rhodanine unit can be an excellent electron acceptor system for organic dyes to improve the photovoltaic performance. Further improvement of DSSCs with organic sensitizers based on the structure of **TPACR2** by molecular engineering aiming for better photovoltaic performance is in progress.

Acknowledgments

This work was financially supported by the National Basic Research Program of China under Grant No. 2011CBA00700, the National Natural Science Foundation of China under Grant Nos. (21003130, 21171084 and 21173227) and the External Cooperation Program of the Chinese Academy of Sciences under Grant No. GJHZ1220.

References

[1] Ito S, Miura H, Uchida S, Takata M, Sumioka K, Liska P, et al. High-conversion-efficiency organic dye-sensitized solar cells with a novel indoline dye. Chem Commun 2008;(41):5194–6.
[2] Matsui M, Inoue T, Ono M, Kubota Y, Funabiki K, Jin JY, et al. Application of novel N-(p-phenylene)-dicyanovinylidene double rhodanine indoline dye for zinc oxide dye-sensitized solar cell. Dyes Pigments 2013;96(2):614–8.
[3] Horiuchi T, Miura H, Sumioka K, Uchida S. High efficiency of dye-sensitized solar cells based on metal-free indoline dyes. J Am Chem Soc 2004;126(39):12218–9.
[4] Koops SE, Barnes PRF, O'Regan BC, Durrant JR. Kinetic competition in a coumarin dye-sensitized solar cell: injection and recombination limitations upon device performance. J Phys Chem C 2010;114(17):8054–61.
[5] Wang Z-S, Cui Y, Dan-oh Y, Kasada C, Shinpo A, Hara K. Molecular design of coumarin dyes for stable and efficient organic dye-sensitized solar cells. J Phys Chem C 2008;112(43):17011–7.
[6] Geiger T, Kuster S, Yum JH, Moon SJ, Nazeeruddin MK, Grätzel M, et al. Molecular design of unsymmetrical squaraine dyes for high efficiency conversion of low energy photons into electrons using TiO_2 nanocrystalline films. Adv Funct Mater 2009;19(17):2720–7.
[7] Kim S, Mor GK, Paulose M, Varghese OK, Baik C, Grimes CA. Molecular design of near-IR harvesting unsymmetrical squaraine dyes. Langmuir 2010;26(16):13486–92.
[8] Chen X, Guo J, Peng X, Guo M, Xu Y, Shi L, et al. Novel cyanine dyes with different methine chains as sensitizers for nanocrystalline solar cell. J Photochem Photobiol A Chem 2005;171(3):231–6.
[9] Edvinsson T, Li C, Pschirer N, Schöneboom J, Eickemeyer F, Sens R, et al. Intramolecular charge-transfer tuning of perylenes: spectroscopic features and performance in dye-sensitized solar cells. J Phys Chem C 2007;111(42):15137–40.
[10] Li C, Yum JH, Moon SJ, Herrmann A, Eickemeyer F, Pschirer N, et al. An improved perylene sensitizer for solar cell applications. ChemSusChem 2008;1(7):615–8.
[11] Zeng W, Cao Y, Bai Y, Wang Y, Shi Y, Zhang M, et al. Efficient dye-sensitized solar cells with an organic photosensitizer featuring orderly conjugated ethylenedioxythiophene and dithienosilole blocks. Chem Mater 2010;22(5):1915–25.
[12] Shi J, Chen J, Chai Z, Wang H, Tang R, Fan K, et al. High performance organic sensitizers based on 11,12-bis(hexyloxy) dibenzo[a,c]phenazine for dye-sensitized solar cells. J Mater Chem 2012;22(36):18830–8.
[13] Srinivas K, Sivakumar G, Ramesh Kumar C, Ananth Reddy M, Bhanuprakash K, Rao VJ, et al. Novel 1,3,4-oxadiazole derivatives as efficient sensitizers for dye-sensitized solar cells: a combined experimental and computational study. Synth Met 2011;161(15–16):1671–81.
[14] Kim M-J, Yu Y-J, Kim J-H, Jung Y-S, Kay K-Y, Ko S-B, et al. Tuning of spacer groups in organic dyes for efficient inhibition of charge recombination in dye-sensitized solar cells. Dyes Pigments 2012;95(1):134–41.
[15] Wang Z-S, Koumura N, Cui Y, Miyashita M, Mori S, Hara K. Exploitation of ionic liquid electrolyte for dye-sensitized solar cells by molecular modification of organic-dye sensitizers. Chem Mater 2009;21(13):2810–6.
[16] Srinivas K, Kumar CR, Reddy MA, Bhanuprakash K, Rao VJ, Giribabu L. D–π–A organic dyes with carbazole as donor for dye-sensitized solar cells. Synth Met 2011;161(1–2):96–105.
[17] Wan ZQ, Jia CY, Zhou LL, Huo WR, Yao XJ, Shi Y. Influence of different arylamine electron donors in organic sensitizers for dye-sensitized solar cells. Dyes Pigments 2012;95(1):41–6.
[18] Hao Y, Yang X, Cong J, Tian H, Hagfeldt A, Sun L. Efficient near infrared D–π–A sensitizers with lateral anchoring group for dye-sensitized solar cells. Chem Commun 2009;(27):4031–3.
[19] Cheng M, Yang XC, Li JJ, Chen C, Zhao JH, Wang Y, et al. Dye-sensitized solar cells based on a donor–acceptor system with a pyridine cation as an electron-withdrawing anchoring group. Chem Eur J 2012;18(50):16196–202.
[20] Yang C-J, Chang YJ, Watanabe M, Hon Y-S, Chow TJ. Phenothiazine derivatives as organic sensitizers for highly efficient dye-sensitized solar cells. J Mater Chem 2012;22(9):4040–9.
[21] Chen C, Liao J-Y, Chi Z, Xu B, Zhang X, Kuang D-B, et al. Metal-free organic dyes derived from triphenylethylene for dye-sensitized solar cells: tuning of the performance by phenothiazine and carbazole. J Mater Chem 2012;22(18):8994–9005.
[22] Tian H, Yang X, Chen R, Pan Y, Li L, Hagfeldt A, et al. Phenothiazine derivatives for efficient organic dye-sensitized solar cells. Chem Commun 2007;(36):3741–3.
[23] Hua Y, Chang S, Huang D, Zhou X, Zhu X, Zhao J, et al. Significant improvement of dye-sensitized solar cell performance using simple phenothiazine-based dyes. Chem Mater 2013;25(10):2146–53.
[24] Karlsson M, Yang L, Karlsson MK, Sun L, Boschloo G, Hagfeldt A. Phenoxazine dyes in solid-state dye-sensitized solar cells. J Photochem Photobiol A Chem 2012;239(0):55–9.
[25] Tian H, Yang X, Cong J, Chen R, Liu J, Hao Y, et al. Tuning of phenoxazine chromophores for efficient organic dye-sensitized solar cells. Chem Commun 2009;(41):6288–90.
[26] Choi H, Baik C, Kang S, Ko J, Kang MS, Nazeeruddin M, et al. Highly efficient and thermally stable organic sensitizers for solvent-free dye-sensitized solar cells. Angew Chem Int Ed 2008;47(2):327–30.
[27] Xu M, Wenger S, Bala H, Shi D, Li R, Zhou Y, et al. Tuning the energy level of organic sensitizers for high-performance dye-sensitized solar cells. J Phys Chem C 2009;113(7):2966–73.
[28] Wan Z, Jia C, Duan Y, Zhang J, Lin Y, Shi Y. Effects of different acceptors in phenothiazine–triphenylamine dyes on the optical, electrochemical, and photovoltaic properties. Dyes Pigments 2012;94(1):150–5.
[29] Shi J, Chai ZF, Zhong C, Wu WJ, Hua JL, Dong YQ, et al. New efficient dyes containing tert-butyl in donor for dye-sensitized solar cells. Dyes Pigments 2012;95(2):244–51.
[30] Wan ZQ, Jia CY, Zhang JQ, Duan YD, Lin Y, Shi Y. Triphenylamine-based starburst dyes with carbazole and phenothiazine antennas for dye-sensitized solar cells. J Power Sources 2012;199:426–31.
[31] Ning Z, Zhang Q, Wu W, Pei H, Liu B, Tian H. Starburst triarylamine based dyes for efficient dye-sensitized solar cells. J Org Chem 2008;73(10):3791–7.
[32] Tang J, Wu W, Hua J, Li J, Li X, Tian H. Starburst triphenylamine-based cyanine dye for efficient quasi-solid-state dye-sensitized solar cells. Energy Environ Sci 2009;2(9):982–90.
[33] Nazeeruddin MK, Zakeeruddin SM, Humphry-Baker R, Jirousek M, Liska P, Vlachopoulos N, et al. Acid-base equilibria of (2,2′-bipyridyl-4,4′-dicarboxylic acid)ruthenium(II) complexes and the effect of protonation on charge-transfer sensitization of nanocrystalline titania. Inorg Chem 1999;38(26):6298–305.
[34] Grisorio R, De Marco L, Allegretta G, Giannuzzi R, Suranna GP, Manca M, et al. Anchoring stability and photovoltaic properties of new $D(-\pi-A)_2$ dyes for dye-sensitized solar cell applications. Dyes Pigments 2013;98(2):221–31.
[35] Abbotto A, Manfredi N, Marinzi C, De Angelis F, Mosconi E, Yum J-H, et al. Di-branched di-anchoring organic dyes for dye-sensitized solar cells. Energy Environ Sci 2009;2(10):1094–101.
[36] Hong YP, Liao JY, Fu JL, Kuang DB, Meier H, Su CY, et al. Performance of dye-sensitized solar cells based on novel sensitizers bearing asymmetric double D–π–A chains with arylamines as donors. Dyes Pigments 2012;94(3):481–9.
[37] Seo KD, You BS, Choi IT, Ju MJ, You M, Kang HS, et al. Dual-channel anchorable organic dyes with well-defined structures for highly efficient dye-sensitized solar cells. J Mater Chem A 2013;1(34):9947–53.
[38] Ren X, Jiang S, Cha M, Zhou G, Wang Z-S. Thiophene-bridged double D–π–A dye for efficient dye-sensitized solar cell. Chem Mater 2012;24(17):3493–9.
[39] Sirohi R, Kim DH, Yu S-C, Lee SH. Novel di-anchoring dye for DSSC by bridging of two mono anchoring dye molecules: a conformational approach to reduce aggregation. Dyes Pigments 2012;92(3):1132–7.
[40] Li Q, Shi J, Li H, Li S, Zhong C, Guo F, et al. Novel pyrrole-based dyes for dye-sensitized solar cells: from rod-shape to "H" type. J Mater Chem 2012;22(14):6689–96.
[41] Wu G, Kong F, Li J, Fang X, Li Y, Dai S, et al. Triphenylamine-based organic dyes with julolidine as the secondary electron donor for dye-sensitized solar cells. J Power Sources 2013;243:131–7.
[42] Wu G, Kong F, Li J, Chen W, Fang X, Zhang C, et al. Influence of different acceptor groups in julolidine-based organic dye-sensitized solar cells. Dyes Pigments 2013;99:653–60.
[43] Wu G, Kong F, Li J, Chen W, Zhang C, Chen Q, et al. Julolidine dyes with different acceptors and thiophene-conjugation bridge: design, synthesis and their application in dye-sensitized solar cells. Synth Met 2013;180(0):9–15.
[44] Yang C-H, Chen H-L, Chuang Y-Y, Wu C-G, Chen C-P, Liao S-H, et al. Characteristics of triphenylamine-based dyes with multiple acceptors in application of dye-sensitized solar cells. J Power Sources 2009;188(2):627–34.
[45] Hu L, Dai S, Weng J, Xiao S, Sui Y, Huang Y, et al. Microstructure design of nanoporous TiO_2 photoelectrodes for dye-sensitized solar cell modules. J Phys Chem B 2006;111(2):358–62.
[46] Frisch MJ, Trucks GW, Schlegel HB, Scuseria GE, Robb MA, Cheeseman JR, et al. Gaussian 09, revision C.01. Wallingford, CT: Gaussian Inc.; 2009.